Pore structure of single-wall carbon nanohorn aggregates

ARTICLE *in* CHEMICAL PHYSICS LETTERS · NOVEMBER 2000

Impact Factor: 1.9 · DOI: 10.1016/S0009-2614(00)01152-0

6 AUTHORS, INCLUDING:

F. Kokai
Mie University
101 PUBLICATIONS **2,847** CITATIONS
SEE PROFILE

Sumio Iijima
Meijo University
598 PUBLICATIONS **32,644** CITATIONS
SEE PROFILE

ELSEVIER

24 November 2000

Chemical Physics Letters 331 (2000) 14–20

CHEMICAL PHYSICS LETTERS

www.elsevier.nl/locate/cplett

Pore structure of single-wall carbon nanohorn aggregates

K. Murata [a], K. Kaneko [a,*], F. Kokai [b], K. Takahashi [b], M. Yudasaka [c], S. Iijima [c,d]

[a] *Physical Chemistry, Material Science, Graduate School of Natural Science and Technology, Chiba University, 1-33 Yayoi, Inage, Chiba 263-8522, Japan*

[b] *Laser Research Center, Institute of Research and Innovation, 1201 Takada, Kashiwa, Chiba 277-0861, Japan*

[c] *Japan Science and Technology Corporation, NEC Corporation, 34 Miyukigaoka, Tsukuba 305-8501, Japan*

[d] *Department of Physics, Japan Science and Technology Corporation, Meijo University, 1501 Shiogamaguchi, Tenpaku-ku, Nagoya 468-8502, Japan*

Received 6 July 2000; in final form 25 September 2000

Abstract

Single-wall carbon nanohorn aggregates were characterized by N_2 adsorption at 77 K and 'particle density' measurement using the high pressure He buoyancy method. The single-wall carbon nanohorn aggregate had micropores and its pore volume was 0.11 ml g^{-1}. The particle density was 1.25 g ml^{-1}. The particle density was not equal to the solid density of graphite (2.27 g ml^{-1}), but it agreed within 15% with the density of the single-wall carbon nanohorn estimated using previous TEM data. Hence single-wall carbon nanohorns have closed micropores covered with single graphene walls. According to N_2 adsorption, single-wall carbon nanohorns have a considerably large surface area (308 m^2 g^{-1}) and open microporosity which has been ascribed to the inter-particle aggregate structure, the so-called '*dahlia* flower type structure'.

1. Introduction

Single-wall carbon nanotubes have stimulated great interest in physics and chemistry with a special relevance to potential applications in electron emitters and hydrogen storage materials [1–4]. Iijima et al. synthesized a new type of horn-shaped sheath aggregate of single-wall graphene sheets, which was named single-wall carbon nanohorns (SWNH) [5,6]. SWNHs are associated with each other to form the '*dahlia* flower-like structured aggregate' whose average diameter is about 80 nm. A detailed X-ray diffraction examination showed that the interhorn-wall distance is 0.4 nm, being greater than the interlayer spacing of graphite (0.335 nm [7]). Thus SWNH aggregates should have both microporosity and mesoporosity originating from the above specific structure. Here IUPAC recommends the following classification of pores according to pore width: w: Micropores; $w < 1$ nm and Mesopores; 2 nm $< w <$ 50 nm.

These SWNHs can be produced at about 10 g h^{-1} with laser ablation at room temperature without a metal catalyst. An exact surface characterization of SWNHs can extend the application possibilities to secondary energy storage materials.

* Corresponding author. Fax: +81-43-290-2788.

E-mail address: kaneko@pchem2.s.chiba-u.ac.jp (K. Kaneko).

0009-2614/00/$ - see front matter
PII: S0009-2614(00)01152-0

2. Experimental

The detailed preparation method of SWNH aggregates was reported in the preceding Letter [5]. In this study, we determined the micropore and mesopore structures of SWNH aggregates by the subtracting pore effect (SPE) method [8,9] using a high resolution α_s plot of the N_2 adsorption isotherm at 77 K and also the closed porosity from the particle density using the high pressure He buoyancy method [10,11].

The porosity of the SWNH aggregates was determined volumetrically by the nitrogen adsorption isotherm at 77 K after pretreatment at 423 K and 1 mPa with the volumetric apparatus (Autosorb 1: Quantachrome). The N_2 adsorption isotherm was analyzed by the high resolution α_s plot. The nitrogen adsorption isotherm of the highly crystalline nonporous carbon black (Mitsubishi 4040B) which shows sharp X-ray diffraction patterns was adopted as the standard isotherm, since the SWNH aggregate was composed of highly ordered graphene sheets.

The particle density ρ_p was estimated from the high pressure He buoyancy effect. This effect was measured gravimetrically at 303 K up to 10 MPa by using an electronic micro-balance (Cahn 1100) and pressure transducers (MKS Baratron). The particle density ρ_p (Eqs. (1a) and (1b)) is different from the true density ρ_t (Eqs. (2a) and (2b)) [12]:

$$\rho_p = \frac{m}{V_{solid} + V_{cp}}, \tag{1a}$$

$$\rho_t = \frac{m}{V_{solid}}. \tag{2a}$$

Here m is the mass of the sample, V_{solid} the volume of the solid part, and V_{cp} is the volume of the closed pores. When V_{solid} and V_{cp} are expressed in ml g^{-1}, m is equal to 1. Hence, Eqs. (1a) and (2a) are given by:

$$\rho_p = \frac{1}{V_{solid} + V_{cp}}, \tag{1b}$$

$$\rho_t = \frac{1}{V_{solid}}. \tag{2b}$$

If the sample has closed pores, these two densities do not coincide. The particle density ρ_p of SWNHs provides the volumes of graphene walls V_{solid} and closed pores V_{cp}. Hence, accurate particle density measurement can provide the closed porosity.

The sample weight decreases linearly with the He pressure owing to the buoyancy effect. The slope of the sample weight vs. He pressure can be given by Eq. (3):

$$(\text{slope}) = \frac{d}{dP}\{n_{ex} - \rho_{bulk}(V_{solid} + V_{cp})\}, \tag{3}$$

where P is the pressure, n_{ex} the surface excess mass of He, and ρ_{bulk} is the density of bulk gas phase He. In the linear region of the weight, we can assume that (dn_{ex}/dP) is negligible and He is a perfect gas at 303 K. Then, the slope is given by:

$$(\text{slope}) = -\frac{M_{He}(V_{solid} + V_{cp})}{RT}. \tag{4}$$

Accordingly, the particle density from the buoyancy-pressure relation is obtained by:

$$\rho_p = \frac{1}{V_{solid} + V_{cp}} = -\frac{M_{He}}{RT}\frac{1}{(\text{slope})}, \tag{5}$$

where M_{He} is the molecular weight of helium, R the gas constant, and T is the temperature.

3. Results and discussion

3.1. Open pore structures

The nitrogen adsorption isotherm at 77 K is shown in Fig. 1. The isotherm is of type II of IUPAC classification without an adsorption hysteresis. This observed adsorption isotherm appears to be a representative isotherm of adsorption on a flat surface. The adsorption process on a flat surface can be described by the BET equation. We analyzed this isotherm by the BET method. The resulting c value of the BET equation is very large ($c = 5800$), suggesting that the SWNH aggregate has micropores. Thus, the BET analysis is not suitable for this system. The N_2 adsorption isotherm was analyzed by the SPE method using the α_s-plot in order to prove the presence of pores. The adsorption on the flat surface is expressed by the line passing both the origin and the point at $\alpha_s = 0.5$. The α_s plot is

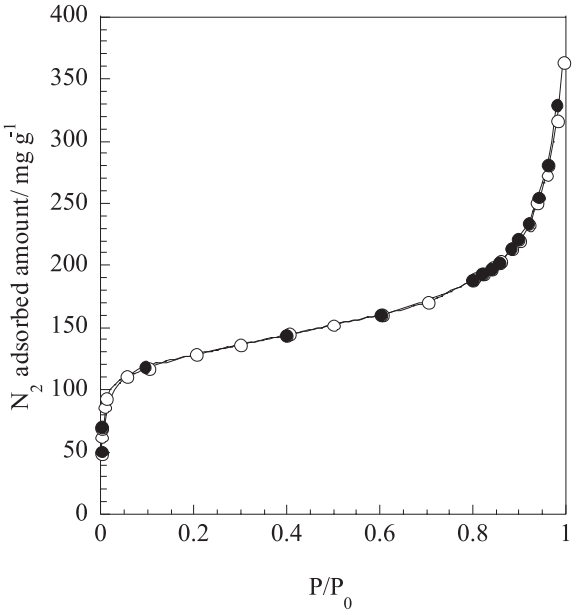

Fig. 1. Nitrogen adsorption isotherm at 77 K on SWNH aggregates; adsorption (○): desorption (●).

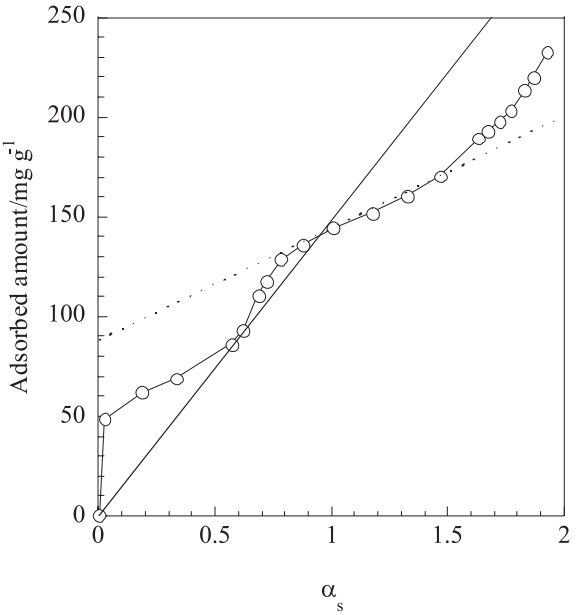

Fig. 2. α_s-plot of nitrogen adsorption isotherm of SWNH aggregates at 77 K. The total surface area and external surface area are obtained from the solid and dotted lines, respectively.

shown in Fig. 2. The deviations from the solid line below $\alpha_s = 1$ are termed as filling swing (FS) and cooperative swing (CS) in the preceding work [13]. The FS and CS come from an enhanced surface–molecule interaction and an attractive interaction by the preformed monolayer, respectively [14]. The FS is associated with primary micropore filling in micropores of pore width $w < 1.0$ nm. On the other hand, the CS stems from cooperative filling in the residual micropore space surrounded by the monolayer-coated walls, whose pore width w is greater than 1.0 nm [15]. The α_s-plot has a large FS and small CS, indicating that SWNH aggregates have a bimodal pore size distribution. The SWNH aggregates have a predominant amount of smaller micropores ($w < 1$ nm) and a small amount of large micropores ($w > 1$ nm). We determined each pore volume from the α_s-plot. The slopes of solid and dotted lines in Fig. 2 lead to the total and external surface areas, respectively. The total pore volume was determined from the ordinate-intercept of the dotted line; the volume of smaller micropores ($w < 1$ nm) was estimated from the adsorbed amount at $\alpha_s = 0.5$ and the volume of the larger micropores ($w > 1$ nm) was obtained from the difference between the total micropore volume and the volume of the smaller pores. As the smaller micropores should stem from wedge-shaped interstices among cylindrical parts of SWNHs, the mean pore width $\langle w \rangle$ was derived by the following simple slit pore approximation:

$$\langle w \rangle = \frac{2W_0}{S - S_{ex}}, \tag{6}$$

where W_0 is the total micropore volume, S the specific surface area, and S_{ex} is the external surface area. The obtained micropore parameters are shown in Table 1. The specific surface area, pore volume of smaller mesopores, and mean average width are 308 $m^2\ g^{-1}$, 0.096 ml g^{-1}, and 1 nm, respectively. This microporosity should be noteworthy.

The deviation from linearity at $\alpha_s = 1.2$ indicates the presence of mesopores regardless of no adsorption hysteresis. The appearance of adsorption hysteresis depends on the geometrical structure of mesopores. For example, test-tube type cylindrical pores give no adsorption hysteresis [15].

Table 1
Microporosity of SWNH aggregates

S	S_{ex}	Total pore volume	Pore volume (ml g^{-1})		$\langle w \rangle$
(m^2 g^{-1})	(m^2 g^{-1})	(ml g^{-1})	$w < 1.0$ nm	$w > 1.0$ nm	nm
308	108	0.11	0.096	0.014	1

Thus, Dollimore–Heal (DH) analysis for the adsorption branch was applied to calculate the mesopore size distribution under the assumption of cylindrical mesopores [16]. The mesopore distribution is shown in Fig. 3. The mesopore size distribution is broad, and it is larger than the size of SWNHs. Hence, the mesopores originate from the aggregated structure of SWNHs. The TEM image [5] supports this idea. As the mesopore size distribution is not sharp, the SWNHs do not necessarily form uniform aggregate structures.

3.2. Closed porosity

The N_2 adsorption at 77 K elucidates the open pore structures, as shown above. The closed porosity is indispensable to understand the structure of SWNH aggregates accurately. The particle density determination using the buoyancy measurement with high pressure helium gas should be helpful to elucidate the closed porosity. The widely used 'helium density', which is based on displacement of an equivalent helium volume at room temperature, is believed to be the true density, since helium adsorption is negligible. However, this assumption is not reliable in the case of microporous solids [17,18]. In fact, Malbrunot et al. [19] showed in their high pressure experiments that the adsorbed helium significantly influences the value of the helium density. Also the true density must be strictly distinguished from the particle density. The particle density takes into account the closed pores, as mentioned before. Hence, we determined the particle density using the high pressure He buoyancy method, as shown in Fig. 4. At the beginning, the sample weight rises beyond zero slightly due to adsorption of helium in micropores, and then decreases linearly with the pressure. The weight decrease comes from the buoyancy and thereby this linear relation can provide the correct slope leading to the particle density, as mentioned

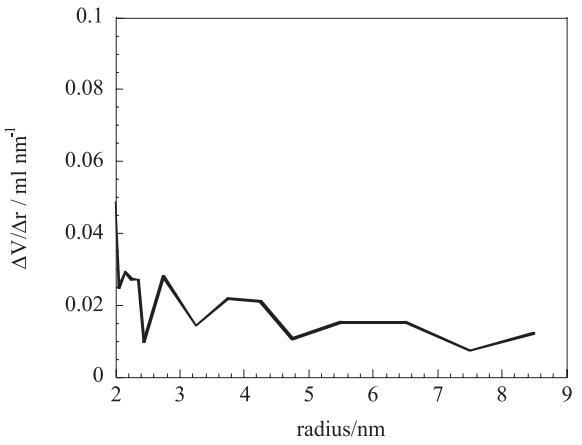

Fig. 3. Mesopore size distribution of SWNH aggregates by using the DH method.

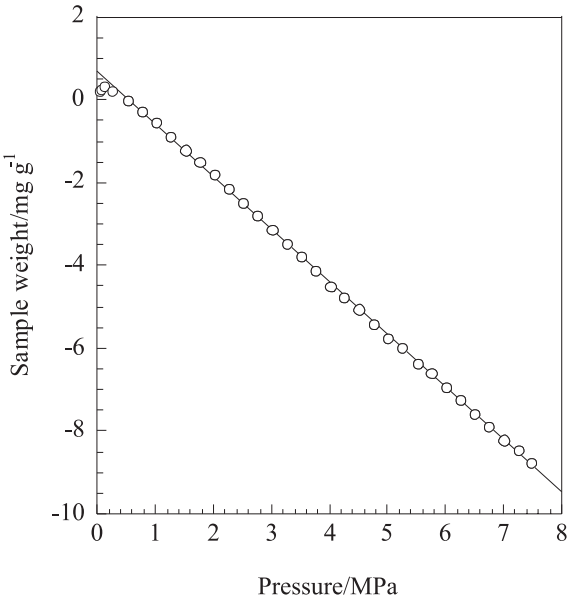

Fig. 4. The buoyancy change of the SWNH sample with helium pressure at 303 K.

before. The obtained particle density is 1.25 g ml^{-1}, being much smaller than the solid density of graphite ρ_{gr} (2.27 g ml^{-1}). Consequently, SWNHs have plenty of closed pores. If SWNHs have no open pores, we can estimate the closed porosity from the geometrical calculation. Table 2 lists the geometrically calculated density, ρ_{geo}, of SWNHs together with the particle density and the solid graphite density. The ρ_{geo} was obtained by a simple horn shape model consisting of a circular cone and a circular cylinder, as shown in Fig. 5(a). The ρ_{geo} is given by:

$$\rho_{geo} = \frac{\rho_{gr} S_H d}{V_H}, \tag{7}$$

where S_H is the surface area of this model, d the distance of the graphite layer, and V_H is the volume of the model. ρ_{geo} is close to ρ_p, supporting the closed porosity. Consequently, SWNHs have no open porosity. The closed pore volume V_{cp} can be obtained from the particle density using the following relation:

$$V_{cp} = \frac{1}{\rho_p} - \frac{1}{\rho_{gr}}. \tag{8}$$

The closed pore volume is 0.36 ml g^{-1}, being about three times greater than the open micropore volume. Thus, the closed pores of SWNHs are quite important.

Table 2
Density and closed pore volume of SWNH aggregates

ρ_p (g ml^{-1})	ρ_{gra} (g ml^{-1})	ρ_{geo} (g ml^{-1})	V_{cp} (ml g^{-1})	V_{solid} (ml g^{-1})
1.25	2.27	1.45	0.36	0.44

3.3. Origin of open porosity and assembly structure

The particle density measurement showed that the micropores stem from inter-SWNH structures. Here, we compare the microporosity from the adsorption measurement and that calculated with the geometrical model. The geometrical model is shown in Fig. 5(b). This model consists of the circles having a spacing of 0.4 nm, which was shown by X-ray diffraction [6]. The dotted circles

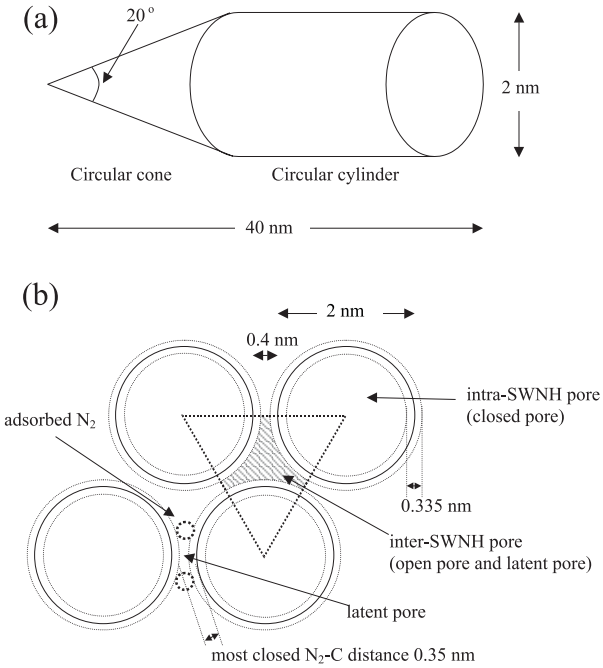

Fig. 5. Geometrical models: (a) The model of the horn. (b) The model of the aggregate structure.

Table 3
The comparison of the assembly structures

Calculation	V_{ap}/V_{op}	V_{cp}/V_{op}	V_{ip}/V_{op}	V_{lp}/V_{op}	V_{solid}/V_{op}
N_2 and He adsorption	7.27	3.27	–	–	4.00
Geometrical model	8.05	3.51	1.14	0.14	3.40

show the surface of rolled graphene and the dotted triangle represents the structure unit. We can calculate microporosity from this two-dimensional geometrical model. The mutual ratio of different pore volumes can be obtained from the ratio of two-dimensional areas. The apparent particle volume V_{ap} contains all kinds of volumes such as the solid volume V_{solid}, the open pore volume V_{op}, the closed pore volume V_{cp}, and the latent pore volume V_{lp}:

$$V_{ap} = V_{solid} + V_{op} + V_{cp} + V_{lp}. \quad (9)$$

Here, the latent pore is an inaccessible pore whose diameter is smaller than that of an adsorbed molecule. Two N_2 molecules are illustrated in Fig. 5(b) in order to show the latent pore. The space between these two N_2 molecules is the latent pore. The area surrounded by three SWNH cylinders, which is illustrated by the hatched lines, corresponds to the volume V_{ip} of inter-SWNH pores. V_{ip} is given by V_{op} and V_{lp}:

$$V_{ip} = V_{op} + V_{lp}. \quad (10)$$

We can calculate the ratio of V_x/V_{op}, where $[x]$ means [ap], [solid], [cp], [lp], or [ip] using the above relations. As V_{ap}/V_{op}, V_{cp}/V_{op}, and V_{solid}/V_{op} can be determined from N_2 adsorption and particle density data, the calculated ratios are compared with the observed ones in Table 3. The calculated ratios agree well with the observed ones irrespective of the simple geometrical model. Accordingly this geometrical model structure of SWNH aggregates should hold basically, as suggested by TEM and X-ray diffraction examinations in the preceding Letters [5,6].

4. Conclusion

The observed closed porosity from the particle density agrees with the structure of SWNHs observed by TEM in the preceding article [6]. The SWNH aggregates have a considerable capacity of micropores of about 1 nm in pore width and a little mesoporosity due to the hexagonal stacking structure of the SWNHs.

Acknowledgements

This work was funded by Grant-in-Aid for Scientific Research B from the Japanese Government.

References

[1] S. Iijima, T. Ichihashi, Nature 363 (1993) 603.
[2] T.W. Odom, J.-L. Huang, P. Kim, C.M. Lieber, Nature 391 (1998) 62.
[3] J.W.G. Wildoer, I.C. Venema, A.G. Rinzler, R.E. Smalley, C. Dekker, Nature 391 (1998) 59.
[4] A.C. Dillon, K.M. Jones, T.A. Bekkedahl, C.H. Kiang, D.S. Bethune, M.J. Heben, Nature 386 (1997) 377.
[5] S. Iijima, M. Yudasaka, R. Yamada, S. Bandow, K. Suenaga, F. Kokai, K. Takahashi, Chem. Phys. Lett. 309 (1999) 165.
[6] S. Bandow, F. Kokai, K. Takahashi, M. Yudasaka, L.C. Qin, S. Iijima, Chem. Phys. Lett. 321 (2000) 514.
[7] W.A. Steele, The Interaction of Gases with Solid Surface, Pergamon, Oxford, 1974.
[8] K. Kaneko, C. Ishii, Colloid Surface 67 (1992) 203.
[9] N. Setoyama, T. Suzuki, K. Kaneko, Carbon 36 (1998) 1459.
[10] K. Kaneko, K. Shimizu, T. Suzuki, J. Chem. Phys. 97 (1992) 8705.
[11] K. Murata, K. Kaneko, Chem. Phys. Lett. 321 (2000) 342.
[12] M. Ruike, T. Kasu, N. Setoyama, T. Suzuki, K. Kaneko, J. Phys. Chem. 98 (1994) 9594.
[13] K. Kaneko, C. Ishii, M. Ruike, H. Kuwabara, Carbon 30 (1992) 1075.
[14] T. Ohba, T. Suzuki, K. Kaneko, Chem. Phys. Lett. 326 (2000) 158.
[15] S.J. Gregg, K.S.W. Sing, Adsorption Surface Area and Porosity, second edn., Academic Press, New York, 1982.
[16] D. Dollimore, G.R. Heal, J. Appl. Chem. 14 (1964) 109.

[17] F.A.P. Maggs, P.H. Schwabe, J.H. Williams, Nature 186 (1960) 956.
[18] F. Rouquerol, J. Rouquerol, K.S.W. Sing, Adsorption by Powders and Porous Solids, Academic Press, New York, 1999.
[19] P. Malbrunot, D. Vidal, J. Vermesse, R. Chahine, T.K. Bose, Langmuir 13 (1997) 539.